

## Comparison of Residual Stresses and Mechanical Properties of Unconventionally Welded Steel Plates

ČAPEK J.<sup>1,a</sup>, TROJAN K.<sup>1,b</sup>, KEC J.<sup>2,c</sup>, ČERNÝ I.<sup>2,d</sup>, GANEV N.<sup>1,e</sup>,  
KOLAŘÍK K.<sup>1,f</sup>, NĚMEČEK S.<sup>3,g</sup>

<sup>1</sup>Department of Solid State Engineering, Faculty of Nuclear Sciences and Physical Engineering, Czech Technical University in Prague, Trojanova 13, 120 00 Prague, Czech Republic

<sup>2</sup>SVÚM a.s., Tovární 2053, 250 88 Čelákovice, Czech Republic

<sup>3</sup>RAPTECH s.r.o., U Vodárny 473, 330 08 Zruč-Senec, Czech Republic

<sup>a</sup>jiri.capek@fjfi.cvut.cz, <sup>b</sup>karel.trojan@fjfi.cvut.cz, <sup>c</sup>kec@svum.cz, <sup>d</sup>ivo.cerny@seznam.cz,  
<sup>e</sup>nikolaj.ganev@fjfi.cvut.cz, <sup>f</sup>kamil.kolarik@fjfi.cvut.cz, <sup>g</sup>nemecek@raptech.cz

**Keywords:** Unconventional welding, X-ray diffraction, Residual stresses, Real structure, High-cycle fatigue

**Abstract.** The paper contains results of macroscopic residual stresses and high-cycle fatigue life of unconventionally welded steel plates. Generally, the manufacturing processes of a machine component introduce residual stresses that have an important and may have even essential influence on their behaviour during service life. Therefore, the goal of this contribution was to compare laser and electron weld concerning the distribution of surface macroscopic residual stresses and high-cycle fatigue life. The results, important for further applications of the used technology, are discussed particularly from the viewpoint of possible critical areas near the welds and their impact on fatigue loading.

### Introduction

Welding is a widely used method for joining materials in production of ships, trains, steel bridges, pressure vessels, etc. Therefore, high demands are laid on mechanical properties and durability of welds used to connect two or more components. However, because of the heterogeneous application of energy and localized fusion, which occur during the welding process, high undesirable residual stresses (RS) can be present in the region near weld and also in the weld itself. These RS occur as a result of the superposition of thermal (tensile effect) and transformation (compressive effect) stresses, see Fig. 1, and could reach high values and subsequently could cause fatigue life reduction or promote of brittle fractures [1]. Therefore, it is necessary to reduce RS values and size of the area affected by the welding. These RS, microstructure and mechanical properties of the weld can be affected by the used welding method, parameters, and the treatment of the material before and after welding.

The state of residual stress across the laser and electron welds was examined using X-ray diffraction. Unconventional welding methods that bring less heat into the weld and surrounding material and therefore less affect the mechanical properties of the material have been compared. They also show high productivity and automation capability compared to manual welding [2]. In this paper, butt welds made of P355 and P460 steel plates for high-pressure vessels were analysed.

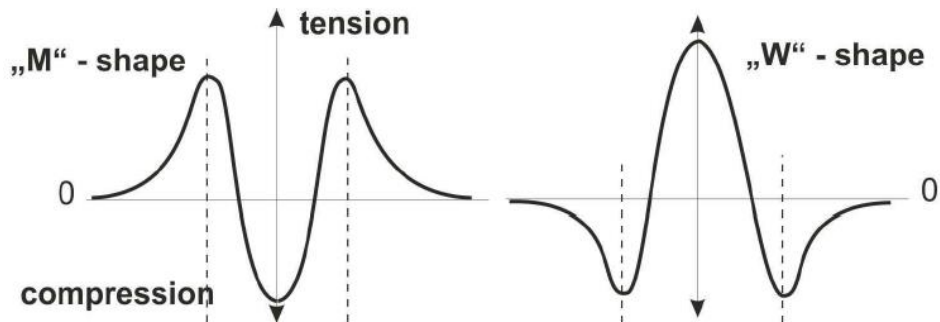


Fig. 1: Characteristic shapes of RS distributions in welds depending on the distance from the weld axis in the perpendicular (left) and parallel (right) direction to the weld [2]

## Experiment

The material studied in this work was P355NL1 and P460NL1 low carbon alloy steel formed into the plates 300×300×20 mm in size. These fine-grained ferritic-perlitic steels are widely used for fabrication of high-pressure vessels, steam boiler parts, pressure piping, compressors, etc. The laser and electron beam welded samples were prepared using a high-power diode laser by the company RAPTECH s.r.o. and at Faculty of Materials Science and Technology in Trnava, respectively. For welding parameters, see Tab. 1. Laser welded plates were machined into the double V-groove shape, see Fig. 2. In the middle part of thickness, the plates were double-side welded, where top sides “U” were welded as the first and bottom sides “D” as the second one. Further, the V-shape groove with a depth of 6 mm was filled with filling wire. Plates welded by the electron beam were joined (single-side weld, where top sides “U” were welded) without filling wire.

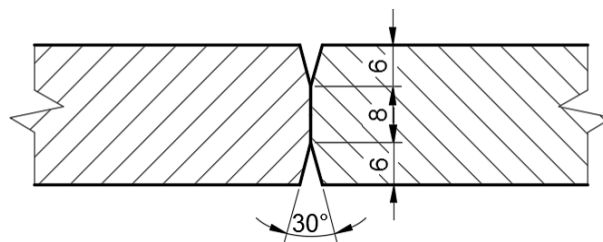


Fig. 2: The double V-groove shape of laser welded plates

Table 1: Welding parameters;  $P$  – power of laser beam,  $v$  – speed of welding,  $\lambda$  – wavelength of laser beam,  $U$  – voltage,  $I$  – current

	$P$ [W]	$v$ [mm·s <sup>-1</sup> ]	mode	$\lambda$ [nm]	$U$ [kV]	$I$ [mA]
laser	3000	5.5	Continuous	900–1080	-	-
electron	-	30	-	-	55	220

The chemical composition of the used steels, measured on SPECTROMAXx OES analyser, is given in Tab. 2. The results show that both materials are Mn alloyed low carbon steels. The Si content was reduced to the absolute minimum due to its negative effect on Charpy impact test properties at low temperatures. Both sheets of steel revealed high metallurgical purity, which resulted in a low content of inclusions. Nevertheless, the measured chemical composition meets the requirements for P355NL1 and P460NL1 steels. The tensile test was carried out at room temperature using the EUS 40 testing machine. For mechanical properties, see Tab. 3.

Table 2: Chemical composition of P355NL1 and P460NL1 steels, in wt%

	C	Si	Mn	P	S	N	Cu	Mo	Cr	Ni	V
P355NL1	0.11	-	0.81	0.016	0.007	-	0.021	-	0.025	0.019	-
P460NL1	0.12	-	1.22	0.015	0.008	-	0.019	-	0.017	0.013	0.041

Table 3: Mechanical properties of laser welded plates of the P355 and P460 steels

Designation	Material	$R_m$	$KV_2$ $0^\circ C$
[-]	[-]	[MPa]	[J]
P355	P355NL1	562	66
P460	P460NL1	624	51

The microstructure of both steels consists of polygonal ferrite and perlite. P355NL1 steel contains a higher volume fraction of perlite in the structure and also the size of the ferritic grains is coarser, which translates into yield strength and brittle fracture properties, as finer grains result in an increase in yield strength and lower DBTT (Ductile-to-Brittle Transition Temperature). The mean grain size of P355NL1 and P460NL1 is  $5.7 \mu m$  and  $3.8 \mu m$ , respectively. As can be seen in Fig. 7a, along the fusion boundary, the effect of grain coarsening in HAZ was observed. The weld metal microstructure consists of acicular ferrite (AF) and grain boundary ferrite (GBF), see Fig. 3b.

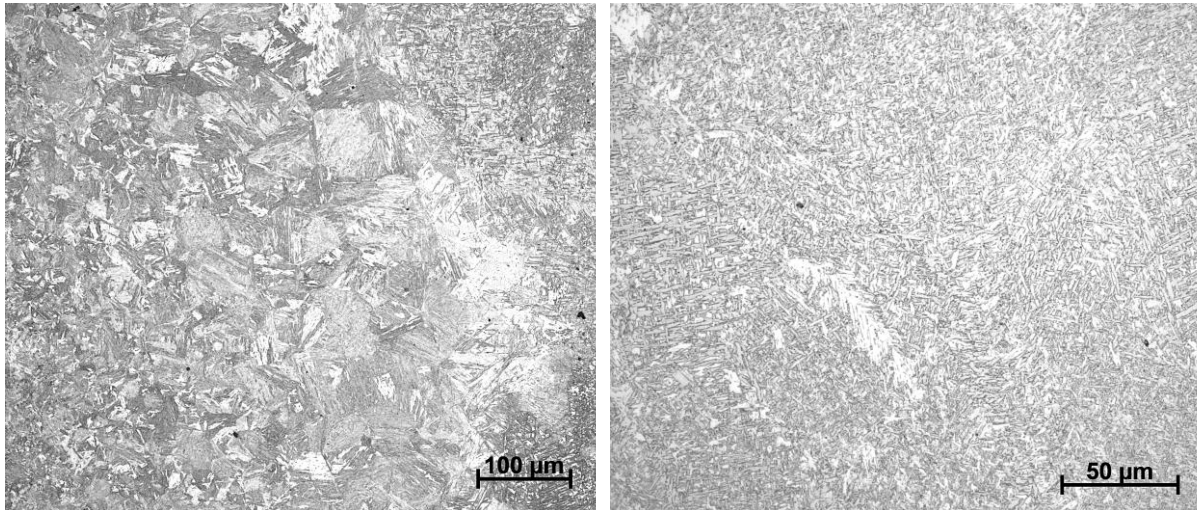


Fig. 3: Microstructure in a) HAZ and b) weld metal

High-cycle fatigue tests were performed at different stress ranges to obtain the whole S-N curve including endurance limit. Load asymmetry was  $R = 0$ , frequency 33 Hz.

The *PROTO iXRD COMBO* diffractometer in  $\omega$ -goniometer set-up with chromium radiation was used for determination of lattice deformations of ferrite phase. Diffraction angles  $2\theta^{hkl}$  were determined using *Gaussian function* and *Absolute peak* method from the peaks of the diffraction lines  $K\alpha_1$  of the  $\{211\}$  planes. To describe the state of RS, the *Winholtz & Cohen* method [3] and X-ray elastic constants  $\frac{1}{2}s_2 = 5.75 \text{ TPa}^{-1}$ ,  $s_1 = -1.25 \text{ TPa}^{-1}$  were used. The samples were analysed in the direction perpendicular “T” and parallel “L” to the welds (welding direction) on both sides of the samples. Welded plates were analysed in the middle part of plates in 18 points ( $x = 0-30 \text{ mm}$  from the axis of the weld). The irradiated area of the primary beam was approx.  $11 \times 1 \text{ mm}$  with the average effective penetration depth of the X-ray radiation approx.  $4 \mu m$  [4].

## Results and discussions

A comparison of RS for both unconventional technologies is presented in Figs. 4 and 5, where L, E, U, and D indicate laser welded specimen, electron beam welded specimen (with thickness of 20 mm), the side which was welded first, and the other side, respectively.

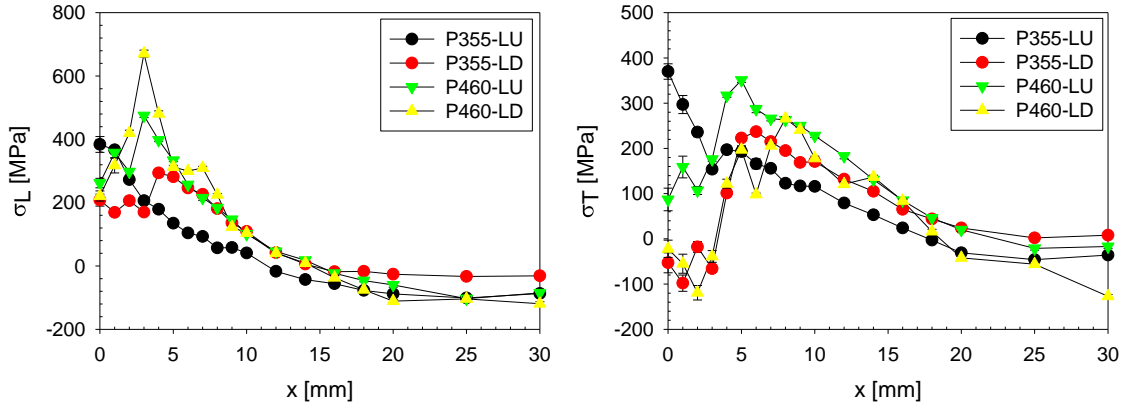


Fig. 4a: Dependence of RS on the distance from the weld axis for the laser weld

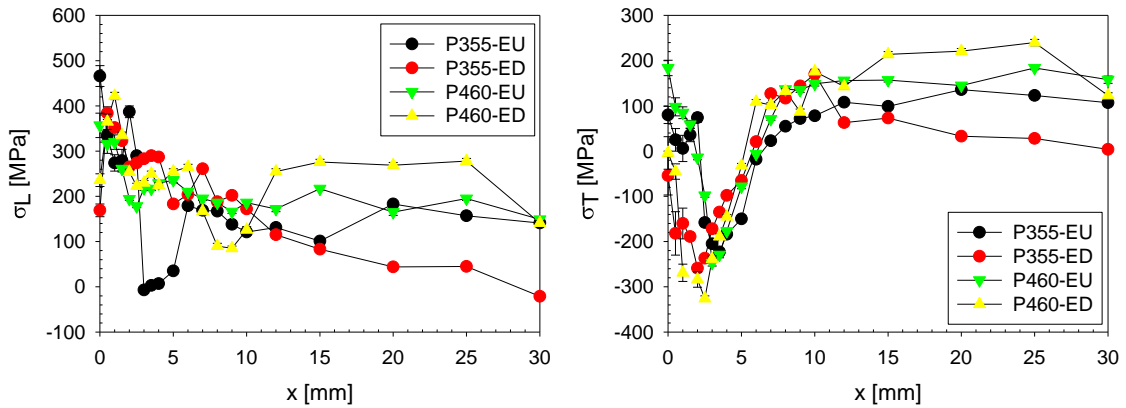


Fig. 4b: Dependence of RS on the distance from the weld axis for the electron beam weld

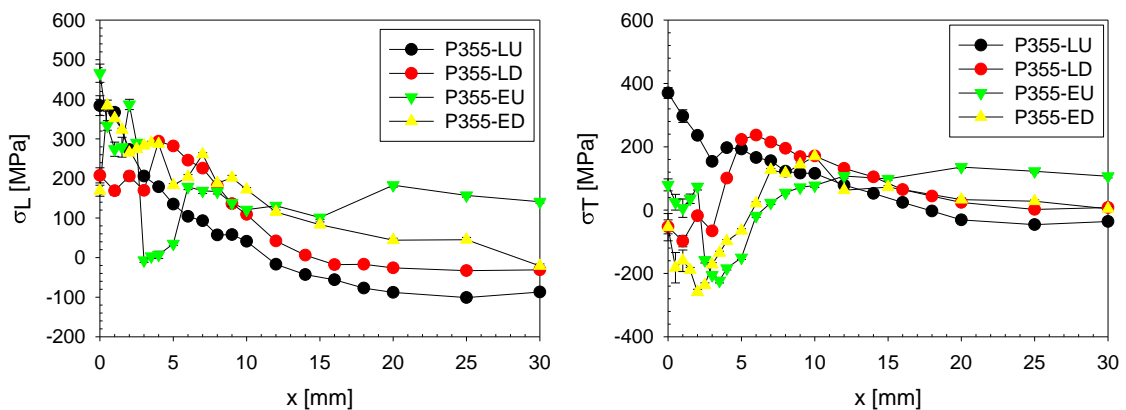


Fig. 5a: Dependence of RS on the distance from the weld axis for P355 steel

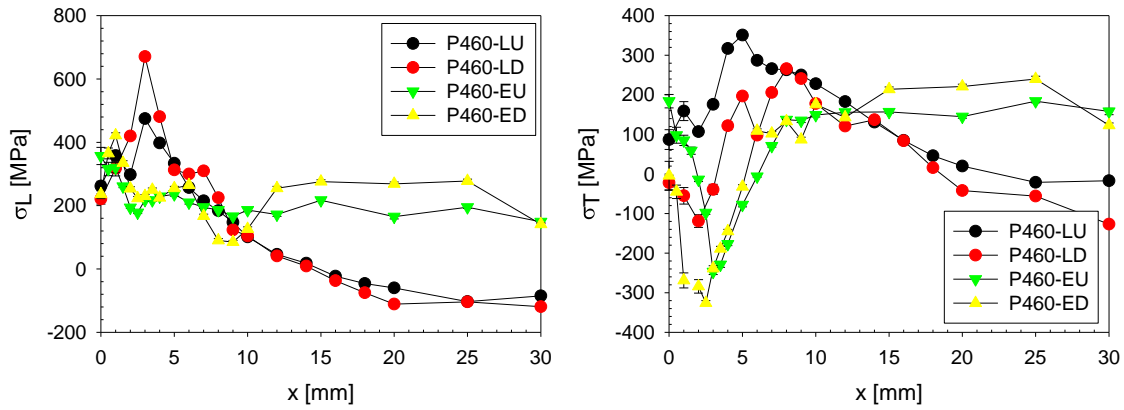


Fig. 5b: Dependence of RS on the distance from the weld axis for P460 steel

From the obtained surface RS profiles, it could be said that there are typical trends of RS on the surface, i.e. tensile RS in the L direction, and both compressive and tensile RS in the T direction, compare Figs. 1 and 4. Nevertheless, higher tensile RS were found for the laser weld on the top side, while lower compressive stresses are on the bottom side, see Fig. 4a. These stresses are probably generated due to the filling of the groove during laser welding and the associated deformation during cooling. RS for electron weld reach higher compressive values in the same area in the T direction. The decreases of RS for electron on the top side at a distance of 3–10 mm in the L direction weld are caused by mechanical removing of the thick oxide layer, see Fig. 4b. The differences in RS values of the bulk material are caused by the steel plates' fabrication, i.e. rolling and/or removing of the thick oxide layer. Analysed RS near the weld are higher than yield strength (approx. 355 MPa and 460 MPa for P355 and P460 steel, respectively), and even than tensile strength  $R_m$  for the laser welded plate of the P460 steel, see Tab. 3 and Figs. 4. This effect could be caused by higher hardness of weld, which would result in different X-ray elastic constants. Heat affected zone (HAZ) for both electron welds is narrower for the bottom side which could result from single-side welding and different amount of heat on each side.

From fatigue life point of view, the surface tensile RS are one of indicator of critical area of possible surface crack initialization. However, the transversal direction T is more important from the technological point of view, in this direction, the main stresses of pressure vessels occur. Unfortunately, unlike electron beam weld, the top side RS in and near laser weld areas in the T direction can be considered as significant from the engineering viewpoint, see Fig. 5.

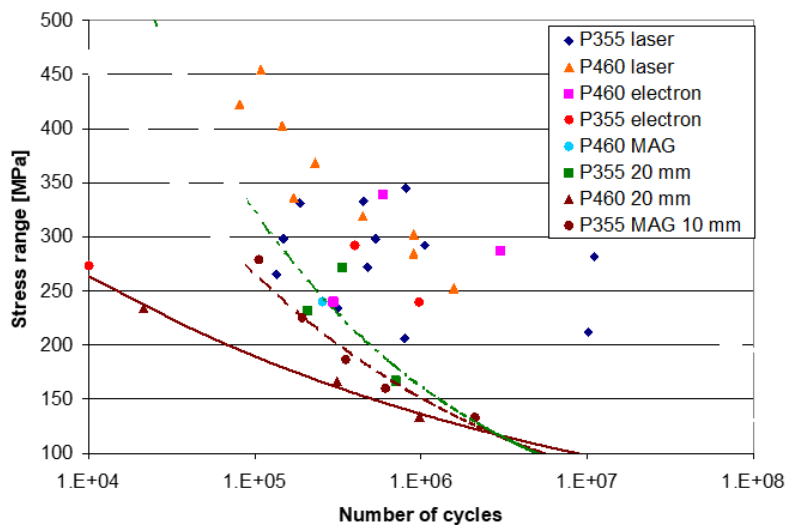


Fig. 6: Results of selected fatigue tests

Results of high-cycle fatigue tests are in Fig. 6, where previous results of investigations performed on welded plates of lower thickness up to 10 mm (single points) are plotted together with S-N curves of 20 mm thick laser welded plates of the P355 and P460 steels and 10 mm thick MAG welded plate of the P355 steel, respectively (points with power regression lines) for a comparison. In general, there are two main groups of points in the diagram. The first group represents tests of plates of the thickness up to 10 mm, mostly between 5–8 mm, welded using either laser or electron beam. If scatter is not considered, particularly in case of the P355 steel caused by internal lack of fusion of some specimens [5], it can be concluded that mean values of fatigue strength are similar. The second group is represented by laser welded plates of 20 mm thickness with fatigue strength incomparably lower indicating that laser welding of thick plates may be problematic and needs special approaches, particularly in case of high strength steels like P460. On the other hand, the results are not so bad in comparison with conventional MAG welding particularly considering that only 10 mm thick plates were evaluated.

What is very important is failure mode of the 20 mm thick laser welded specimens. Fatigue cracking was initiated either in the centre of the welds on internal welding defects or on the specimen surface. In the latter case, all cracking occurred exactly in fusion zone, i.e. at the distance approx. 2 mm from the weld centre. Looking at Fig. 4a, it is clear that cracking did not initiated at the area of maximum tensile RS, the RS were contrarily low or even negative there. As a result of the mentioned internal welding defects, the real cross-sections of investigated specimens were lower in the welds. If the fatigue resistance were re-calculated by considering only the real cross-section of welds without lack of fusion and pores, the correction would result in a significant increase in fatigue resistance. Therefore, the initialization of the surface crack in the fusion zone was caused by a combination of the internal defects (i.e. reduction of the real cross-section of the sample) and small surface compressive or tensile RS.

## Conclusions

From surface RS point of view, the critical area for a potential surface crack initialization was on the top side of both laser welded steels in the weld zone and HAZ. The interface of fusion zone could be most critical because of higher hardness, different microstructure, and the presence of notches.

During laser welding, there was no perfect penetration, especially in the middle part of the weld, which was produced without the filling wire. It is also possible to see that there was a lack of inter-run fusion in the weld beads. The positive finding was that despite the weld discontinuities, the final fracture was localized to the base material during the tensile tests.

Investigations of fatigue properties of laser welded plates of 20 mm thickness showed that fatigue strength was incomparably lower in comparison with previous results of laser welded plates of the thickness up to 10 mm indicating that laser welding of thick plates may be an issue and needs special approaches, particularly in case of high strength steels like P460. Failure mode on the specimen surface exactly in fusion zone was caused by the combination of several effects, mainly low compressive or tensile surface RS and internal weld defects (reduction of the real cross-section).

## **Acknowledgement**

This work was supported by the project TH02010664 of the Technology Agency of the Czech Republic and by the Grant Agency of the Czech Technical University in Prague, grant No. SGS19/190/OHK4/3T/14.

## **References**

- [1] D. Radaj, Heat effects of welding: temperature field, residual stress, distortion, Springer Science & Business Media, 2012.
- [2] T. Nitschke-Pagel, K. Dilger, Sources and consequences of residual stresses due to welding, Mater. Sci. Forum 783 (2014) 2777–2785.
- [3] U. Welzel, J. Ligot, P. Lamparter, A.C. Vermeulen, E.J. Mittemeijer, Stress analysis of polycrystalline thin films and surface regions by X-ray diffraction, J. Appl. Crystallogr. 38 (2005) 1–29.
- [4] J. Čapek, Z. Pala, Programs for Visualizing Results of Diffraction Experiments, Mater. Struct. 22 (2015) 78–81.
- [5] I. Černý, J. Kec, Evaluation of Fatigue Resistance of Laser Welded High Pressure Vessels Steel P355 Considering Fracture Mechanics Approach, Key Eng. Materi. 827 (2019) 428–433.